minerals

MDPI

Article

Gemological and Luminescence Characteristics of Taaffeites from Mogok, Myanmar

Bihan Lin [1], Xingtong Li [1], Longbo Zhang [2], Xiaojing Lai [1] and Qian Zhang [1,*]

[1] Gemological Institute, China University of Geosciences, Wuhan 430074, China
[2] National Center for Quality Inspection and Testing of Gem & Gold-Silver Jewelry (Henan), Henan Institute of Product Quality Supervision and Inspection, Zhengzhou 450047, China
* Correspondence: qianzhang@cug.edu.cn

Abstract: Taaffeite is a rare gem that has been found in different localities such as Tanzania, Sri Lanka, China, and Mogok, Myanmar. In this study, thirty-two taaffeite samples from Mogok, Myanmar, were investigated by conventional gemological testing, laser ablation inductively coupled plasma mass spectrometry (LA-ICP-MS), Raman spectrometry, and fluorescence spectrometry. Through microscopic observations, various types of inclusions were observed in these taaffeites, including irregular inclusions, orange and brown intrusions, black dotted and flake inclusions, healed fissures, tubular inclusions, fingerprint inclusions, and multi-phase inclusions. The Raman spectra demonstrated that the inclusions were mainly calcite, forsterite, celestite, graphite, dolomite, and transparent tubular or columnar inclusions filled with CO_2. In previous studies, taaffeite showed inert or chalky fluorescence under long-wave ultraviolet (LWUV) light and inert fluorescence under short-wave ultraviolet (SWUV) light. In this study, the taaffeite samples revealed different fluorescence phenomena under ultraviolet light. Thirty-two taaffeite samples were classified into four categories according to their fluorescence under LWUV: orange-red, pink, green, and blue-white fluorescence. Under SWUV, all samples presented inert to bright pink fluorescence. Two-dimensional fluorescence spectra were obtained through a fluorescence spectrometer. For the samples with orange-red and pink fluorescence under LWUV, two-dimensional fluorescence spectra showed that peaks at 686 nm and 690 nm (in the red region) were strong. For the samples with green and blue-white fluorescence under LWUV, peaks at 439 nm and 464 nm (in the blue region) were strong, peaks at 507–515 nm (in the green region) were relatively weak, and peaks at 686 and 690 nm (in the red region) were very weak. Combined with the data from LA-ICP-MS, it is speculated that Cr^{3+} was responsible for samples having orange-red and pink fluorescence, that Mn^{2+} was responsible for samples having green fluorescence, and that Fe inhibited the generation of fluorescence.

Keywords: taaffeite; Mogok; gemological characteristics; fluorescence spectroscopy; luminescence

check for updates

Citation: Lin, B.; Li, X.; Zhang, L.; Lai, X.; Zhang, Q. Gemological and Luminescence Characteristics of Taaffeites from Mogok, Myanmar. *Minerals* **2023**, *13*, 346. https://doi.org/10.3390/min13030346

Academic Editor: Evgeny Galuskin

Received: 14 January 2023
Revised: 11 February 2023
Accepted: 27 February 2023
Published: 28 February 2023

Copyright: © 2023 by the authors. Licensee MDPI, Basel, Switzerland. This article is an open access article distributed under the terms and conditions of the Creative Commons Attribution (CC BY) license (https://creativecommons.org/licenses/by/4.0/).

1. Introduction

Taaffeite is one of the rarest gem species in the world. It is an oxide mineral with the chemical formula $BeMg_3Al_8O_{16}$ that belongs to the hexagonal crystal family. Single crystals of taaffeite are usually hexagonal bipyramidal or barrel shaped, and their aggregation is granular.

Taaffeite belongs to the taaffeite group, which has three members: magnesiotaaffeite-2N′2S, magnesiotaaffeite-6N′3S, and ferrotaaffeite-6N′3S [1]. Magnesiotaaffeite-2N′2S is commonly known as taaffeite. The structure of taaffeite (magnesiotaaffeite-2N′2S) is composed of two spinel modules ($T_2M_4O_8$, marked as S) and two modified nolanite modules ($BeTM_4O_8$, marked as N′) [2].

The crystal structure of taaffeite is based on a close-packed oxygen framework and three types of cation layers: O, $T_{1'}$, and T_2. O–T_2 represents a spinel module, and O–$T_{1'}$ represents a modified nolanite module [3]. The whole structure of taaffeite can be defined as –$OT_2OT_{1'}OT_2OT_{1'}$– [4]. Figure 1 shows that the O layer has three octahedrons. In the

$T_{1'}$ layer, there are four octahedrons and two opposite tetrahedrons. The T_2 layer has one octahedron and five tetrahedrons [3,5]. In taaffeite's structure, element occupancies are complicated. Be^{2+} always occupies a tetrahedral site in a $T_{1'}$ layer. Al^{3+} can occupy the octahedral sites in an O layer or a T_2 layer and one of the tetrahedral sites in a $T_{1'}$ layer. Mg^{2+} can be present in tetrahedral sites in a T_2 layer and in octahedral sites in a $T_{1'}$ layer [3]. In addition, trace element substitution exists in taaffeite. For example, Cr^{3+} often replaces Al^{3+} (in 6-coordination) [6]. Zn^{2+}, Fe^{2+}, and Sn^{2+} can replace Mg^{2+} (in 4-coordination) [3].

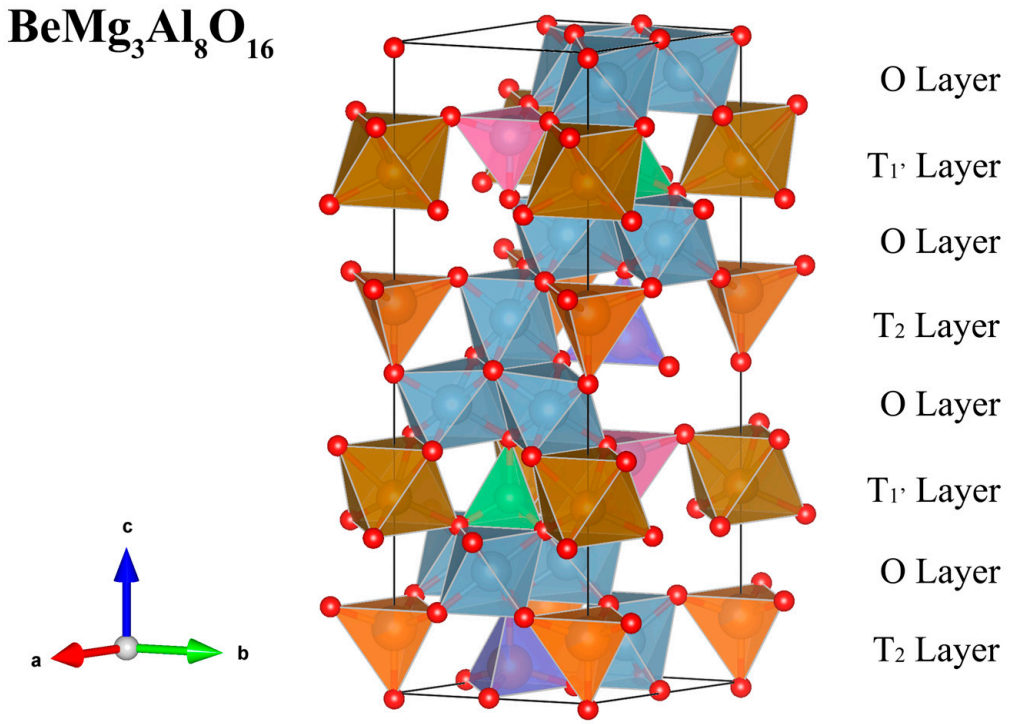


Figure 1. Polyhedral representation of the magnesiotaaffeite-2N'2S crystal structure. The pink and green tetrahedrons in the $T_{1'}$ layers have opposite directions, and the same goes for the orange and purple tetrahedrons in the T_2 layers.

Taaffeite is reportedly produced in Tanzania, Sri Lanka, Myanmar, and China [7–11]. According to previous studies, the refractive index of taaffeite is 1.715–1.735, and its specific gravity is 3.57–3.78 [7–10]. The inclusions in taaffeites from Sri Lanka are zircon, magnesite, feldspar, apatite, muscovite, spinel, phlogopite, fingerprint-like inclusions, healing fissures, and negative crystals with multi-phase inclusions [9,10,12,13]. Healed fissures are seen in taaffeite samples from Myanmar [7]. In general, taaffeite shows inert or chalky fluorescence under long-wave ultraviolet (LWUV) light and inert fluorescence under short-wave ultraviolet (SWUV) light [6,8,10,12].

The Mogok region is located in the middle of the Mogok metamorphic band, which is a significant origin area for gems [14–16]. Systematic research on the taaffeite from Mogok, Myanmar, is still lacking. In this study, thirty-two taaffeites from Mogok were collected. These taaffeite samples were discovered in Ohngaing mine, Mogok Valley, Mogok Township, Pyin-Oo-Lwin District, Mandalay Region, Myanmar. The principal rocks in Ohngaing are syenite, marble, and gneiss [17].

Gemological, luminescence, and chemical characteristic analyses were carried out through conventional gemological testing, laser ablation inductively coupled plasma mass spectrometry (LA-ICP-MS), Raman spectroscopy, and fluorescence spectroscopy. This study can enhance our understanding of taaffeite from Mogok and provide a new research basis for the gems' characteristics.

2. Materials and Methods

2.1. Materials

Thirty-two taaffeites from Mogok, Myanmar were selected for examination (Figure 2). All these samples are small, faceted gems with weights ranging from 0.04 g to 0.51 g. The samples were colorless to light pink with translucent and vitreous lusters due to abundant inclusions.

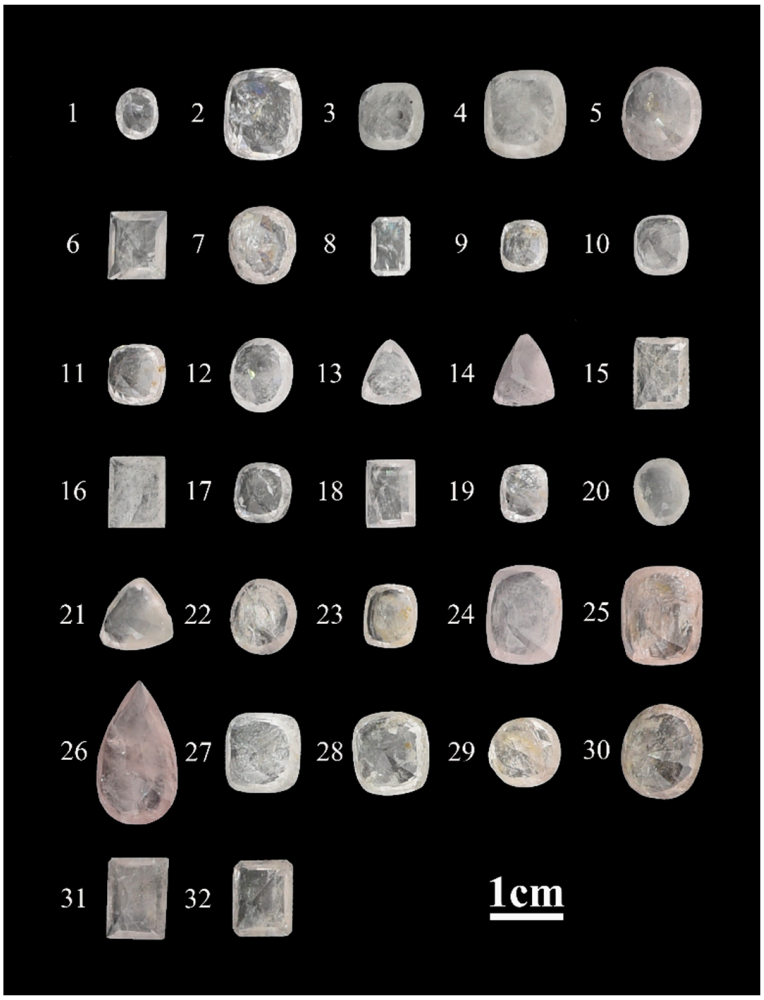


Figure 2. Thirty-two taaffeites from Mogok, Myanmar.

2.2. Methods

Photomicrographs of the inclusions in the samples were taken using a Leica DFC 550-Leica M205 A Microphotographic system in the Gemmological Institute of China University of Geosciences (Wuhan, China).

Raman spectra of all the inclusions in the samples were obtained using a HORIBA LabRAM HR Elolution spectrometer with the following parameters: 532 nm, 600 nm grating, 0–1500 cm^{-1} range. The spectra were collected in the State Key Laboratory of Geological Processes and Mineral Resources, China University of Geosciences (Wuhan, China).

The fluorescence emission spectra of all samples were obtained using a JASCO FP-8500 fluorescence spectrometer (JASCO, Ishikawamachi Hachioji-shi Tokyo, Japan) in the Gemmological Institute of China University of Geosciences (Wuhan, China). The following parameters were used: Ex bandwidth—5 mm, Em bandwidth—2.5 mm, PMT voltage—820 V/720 V (720 V only for samples 16 and 29 with the blue-white fluorescence under LWUV), and scan speed—1000 nm/min. The ultraviolet fluorescent lamp used in this study was tested using a Skyray UV100, and the LW and SW wavelengths were 369 nm

and 254 nm, respectively. Therefore, 369 nm was chosen as the emission wavelength of the two-dimensional fluorescence spectra.

The chemical composition analysis was conducted using a GeoLasPro Agilent 7900a LA-ICP-MS at Wuhan Sample Solution Analytical Technology Co., Ltd., Wuhan, China. The laser beam spot diameter was 44 μm with a frequency of 5 Hz and an intensity of 5.5 J/cm^2. NIST 610, BHVO-2G, BCR-2G, and BIR-1G were used as calibration reference materials. After every six ablated points, the analysis was followed by a calibration of the instrument with NIST 610 in order to correct the time-dependent drift of sensitivity and mass discrimination. The raw data were processed by ICPMS Data Cal software, and the multi-external standards combined internal standard calibration strategy for oxide was used for quantitative calculations. Since the main elements of taaffeite are Be, Mg, Al, and O, Al was chosen as the internal normalizing element to calculate other elements.

Thirty-two samples were analyzed in two parts using LA-ICP-MS for a total of 47 points. In the first test, sample Nos. 2, 14, 15, 16, 17, 23, 24, 25, 26, 27, 28, 29, 30, 31, and 32 were tested at two points, respectively. The element contents of the two points of one sample are similar. The remaining samples (Nos. 1, 3, 4, 5, 6, 7, 8, 9, 10, 11, 12, 13, 18, 19, 20, 21, and 22) were only tested at one point for analysis.

3. Results and Discussion

3.1. Gemological Properties

Thirty-two taaffeite samples had a refractive index of 1.713–1.729 with a birefringence of between 0.001 and 0.006. Specific gravity varied from 3.578 to 3.686. These results are consistent with those of past studies on taaffeite [7–10].

These samples were observed and photographed under visible light and UV light (Figure 3). According to their fluorescence colors under LWUV light, the samples can be divided into four categories: the orange-red, pink, green, and blue-white fluorescence groups. All of them revealed inert to bright pink fluorescence under SWUV light.

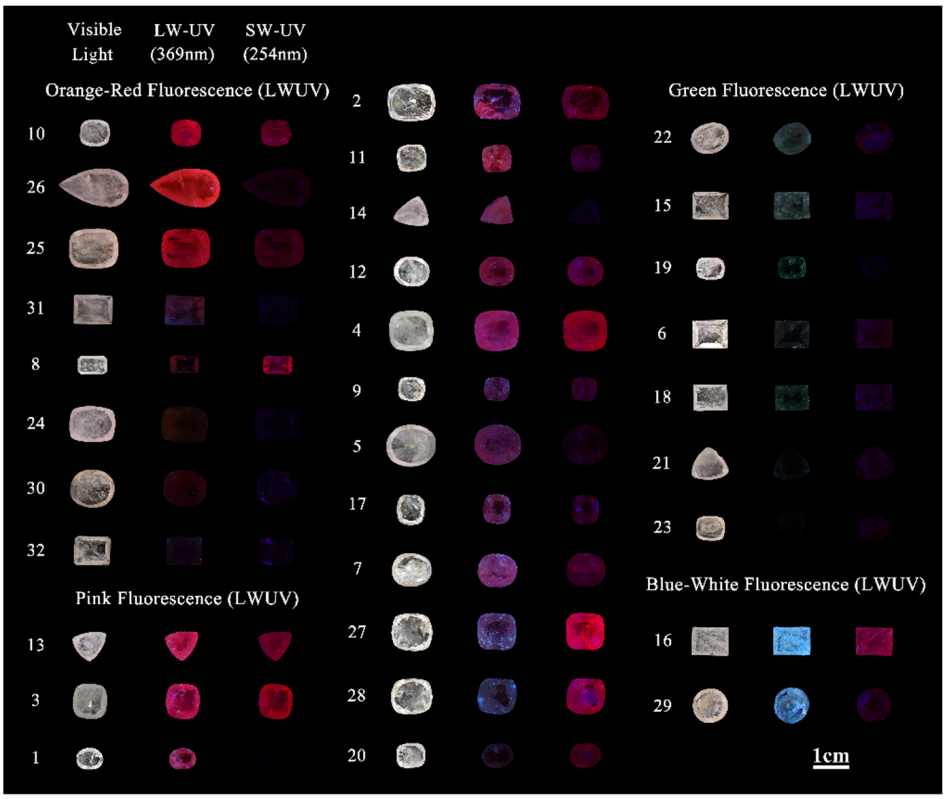


Figure 3. Thirty-two taaffeite samples show different fluorescence under LWUV and SWUV.

Various inclusions were found in these taaffeites. The inclusions can be divided into five types: (1) transparent columnar and irregular inclusions (Figure 4a,b); (2) orange and brown intrusions, mostly filling in the fissures or healed fissures of the host crystal (Figure 4c,d); (3) black punctual and flake inclusions, which occur in large quantities in samples 14 and 16 and are mostly hexagonal plates (Figure 4e,f); (4) fissures and healed fissures (Figure 4g,h); (5) multi-phase inclusions, which are mostly transparent tubes containing black dots or irregular minerals (Figure 4i,j). The irregular inclusions are about 50 μm in length; tubular inclusions are 50–70 μm in length and about 60 μm in width; black inclusions are about 100 μm in length and 10–50 μm in width.

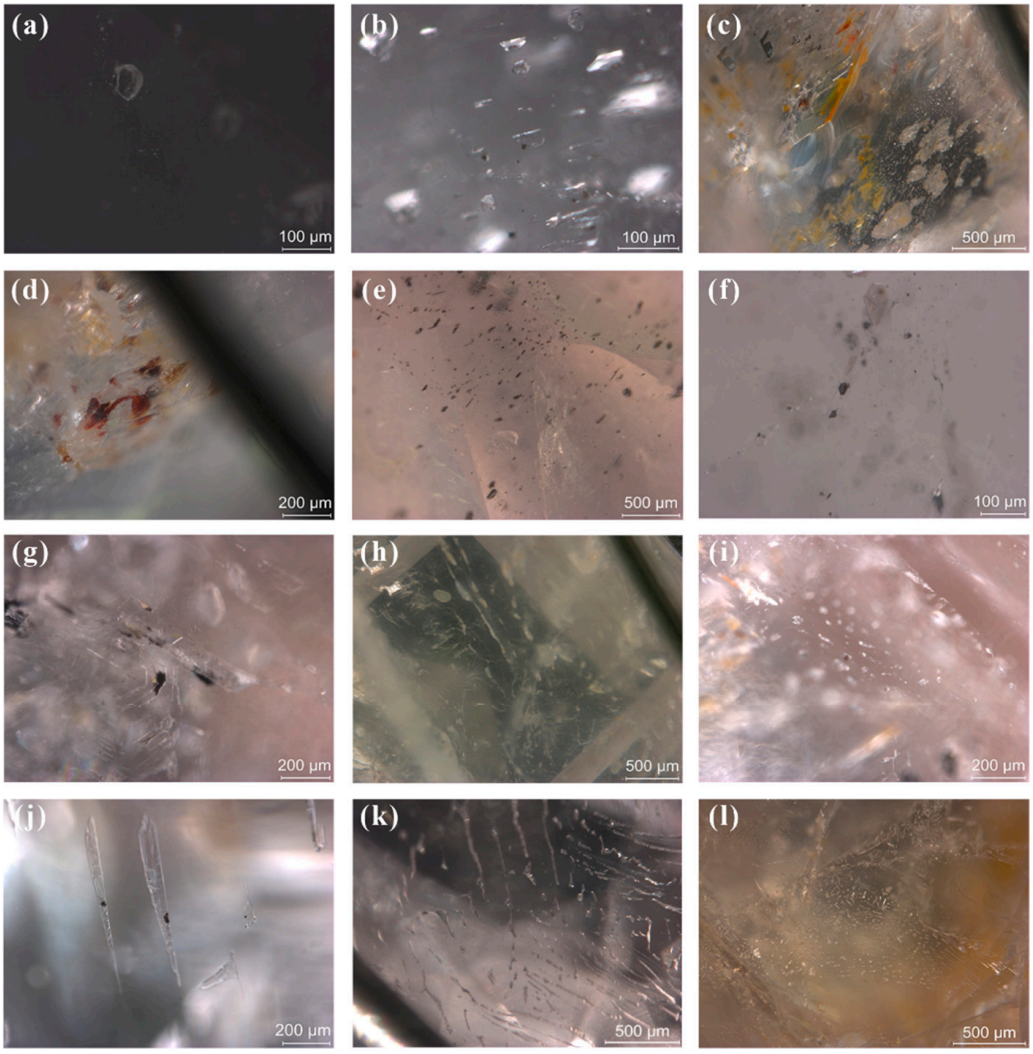


Figure 4. The inclusions in taaffeite samples. (**a**,**b**) irregular inclusions; (**c**,**d**) orange and brown intrusions; (**e**,**f**) black punctual and flake inclusions; (**g**,**h**) healed fissures; (**i**,**j**) multi-phase inclusions; (**k**,**l**) fingerprint-like inclusions (gas-liquid inclusions in healed fissures).

3.2. Identification of the Inclusions

The inclusions of the taaffeite samples were identified by Raman spectroscopy (Figure 5). In some spectra, the peaks at 416–417 cm^{-1}, 436 cm^{-1}, 489 cm^{-1}, 706 cm^{-1}, 715 cm^{-1}, 763 cm^{-1}, and 814 cm^{-1} are the Raman peaks of the host taaffeite [18].

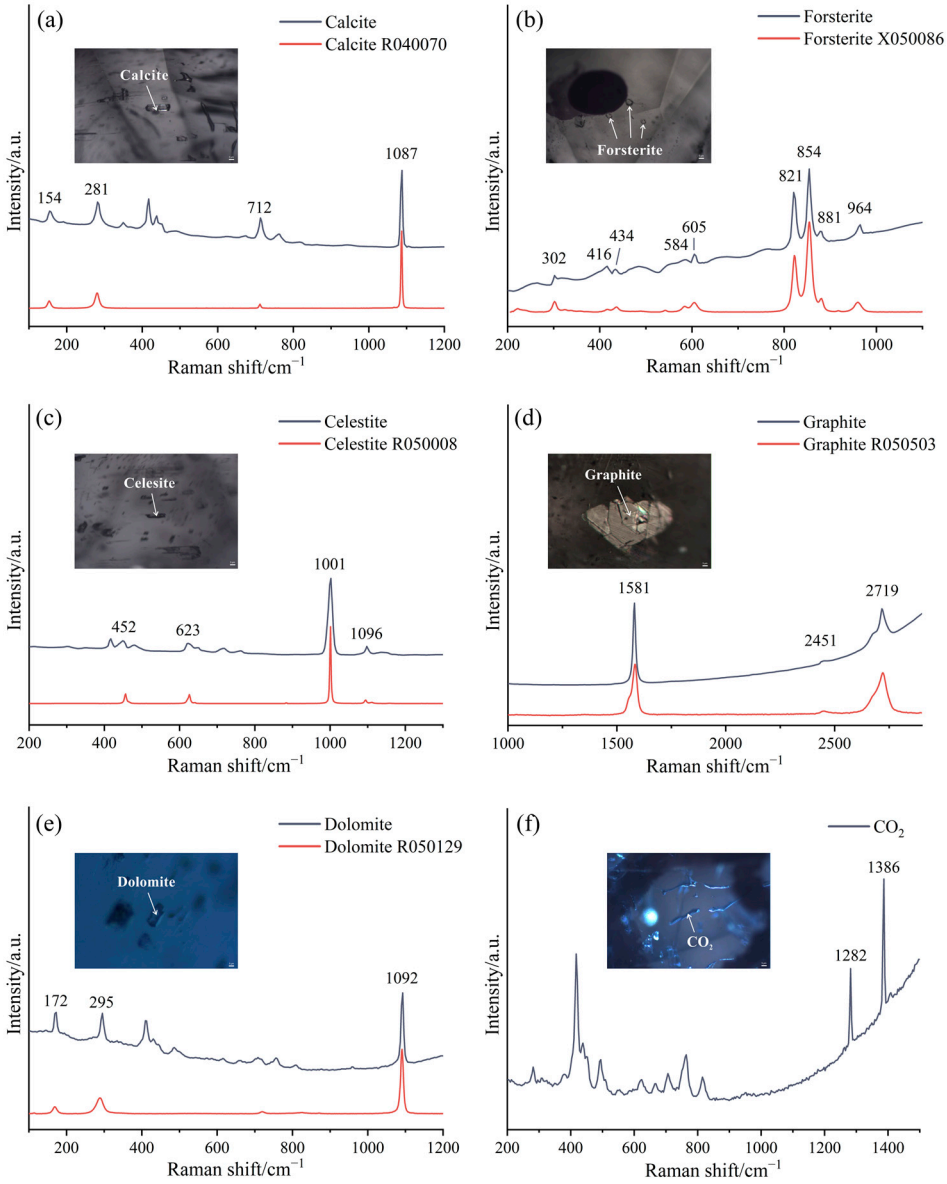


Figure 5. The Raman spectra of inclusions in taaffeite samples. (**a**) calcite; (**b**) forsterite; (**c**) celestite; (**d**) graphite; (**e**) dolomite; (**f**) CO_2. Subfigures in each figures indicated the Raman test locations.

The mineral inclusions of taaffeites were identified as calcite, forsterite, celestite, dolomite, and graphite. In addition, some transparent tubular or columnar inclusions were filled with CO_2. Dolomite was frequently found in the spinel from Mogok, Myanmar [16]. Therefore, dolomite was inferred as a characteristic inclusion of spinel from Mogok, Myanmar. For taaffeite, dolomite may be a typical inclusion in this region, but it has never been found in other areas [8,9,13].

Multi-phase inclusions were found in some samples, which consist of black blocky or irregular crystals wrapped up with transparent columnar, tubular, or irregular crystals. Figure 6a shows a multi-phase inclusion in sample 2, with four black crystals wrapped in an irregular transparent inclusion. Raman spectroscopy indicated that the transparent inclusion was filled with CO_2, while the black inclusions on the right were pyrite. Figure 6b shows another multi-phase inclusion in sample 2, and the transparent tubular inclusion was composed of four different phases. The left part of the multi-phase inclusion was celestite, and the right part is calcite. In the middle, a black pyrite coexists with CO_2.

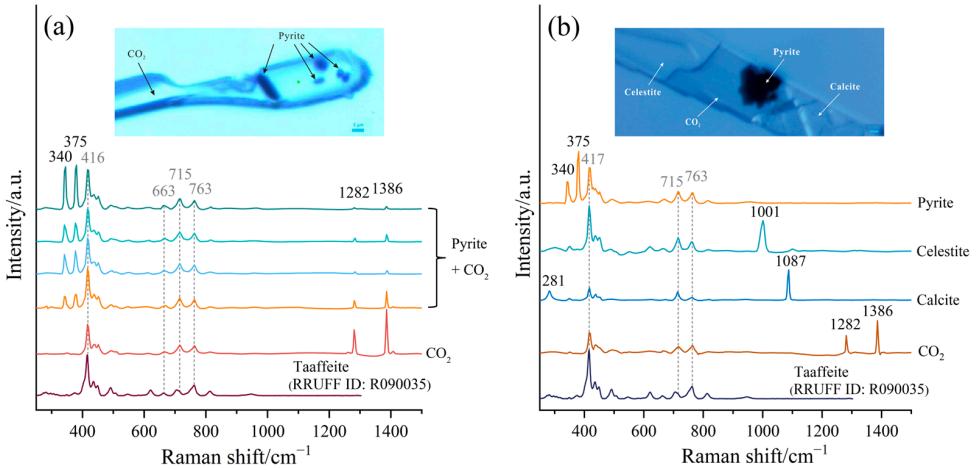


Figure 6. (**a**,**b**) Two multi-phase inclusions in sample 2 and their corresponding Raman spectra (the numbers marked as gray are the Raman peaks of the host taaffeite).

In the taaffeite samples, large amounts of carbonates, i.e., calcite and dolomite, were found. These minerals were also found in Mogok spinels that were produced in the carbonate metamorphic rock [16]. It can be presumed that taaffeite from Mogok was generated in carbonate metamorphic rock.

3.3. Fluorescence Spectroscopy

Mineral luminescence should satisfy the following conditions simultaneously: (1) a lattice type suitable for the formation of emission centers; (2) some fluorescence-producing elements; (3) a relatively small number of quenchants [19]. Transition metal elements are one of the important factors of mineral luminescence. For example, Mn^{2+} is the most popular luminescence agent in nature, and Fe^{3+} is a commonly known quenchant [20]. The red fluorescence in minerals, such as ruby and spinel, is mainly caused by Cr^{3+} [21,22]. Therefore, in this study, the contents of the common transition metal elements (Cr, Ti, V, Mn, and Fe) are compared with the fluorescence color and intensity of taaffeites to analyze their correlation.

3.3.1. Orange-Red and Pink Fluorescence Group under LWUV

Figure 7a shows the two-dimensional fluorescence spectra of samples with orange-red fluorescence under LWUV (No. 8, 10, 24, 25, 26, 30, 31, and 32). The red region was magnified for better analysis (on the left side of Figure 7a).

The fluorescence peaks at 686 nm and 690 nm in the red region are prominent. Combined with two-dimensional fluorescence spectra and the fluorescence image (Figure 3), the samples with apparent orange-red fluorescence under LWUV have strong peaks in the red region (No. 10, 26, and 25). Correspondingly, samples with less obvious fluorescence have weaker peaks (No. 30 and 32).

In Table 1, the trace element data obtained from LA-ICP-MS were analyzed and discussed. Among the samples with orange-red fluorescence under LWUV, samples 10 and 31 have moderate contents of Cr (32.1 ppmw and 43.9 ppmw). However, the contents of Fe, which are 2822 ppmw and 4554 ppmw, are distinctly different. Correspondingly, sample 10 had the strongest and sample 31 had the weak fluorescence (Figure 3). In addition, sample 26 had the highest content of Cr (109 ppmw) and a higher Fe content (3815 ppmw) and weaker fluorescence intensity than sample 10. Therefore, Fe can restrain the production of fluorescence, and taaffeite with high Fe content should have weak fluorescence intensity. For instance, samples 24, 30 and 32 had relatively high contents of Fe (4766 ppmw, 4993 ppmw, and 5098 ppmw, respectively), and their fluorescences were weak. Overall, these results demonstrate that Cr is the activator of orange-red fluorescence in taaffeite under LWUV and that Fe is a powerful quenchant of fluorescence.

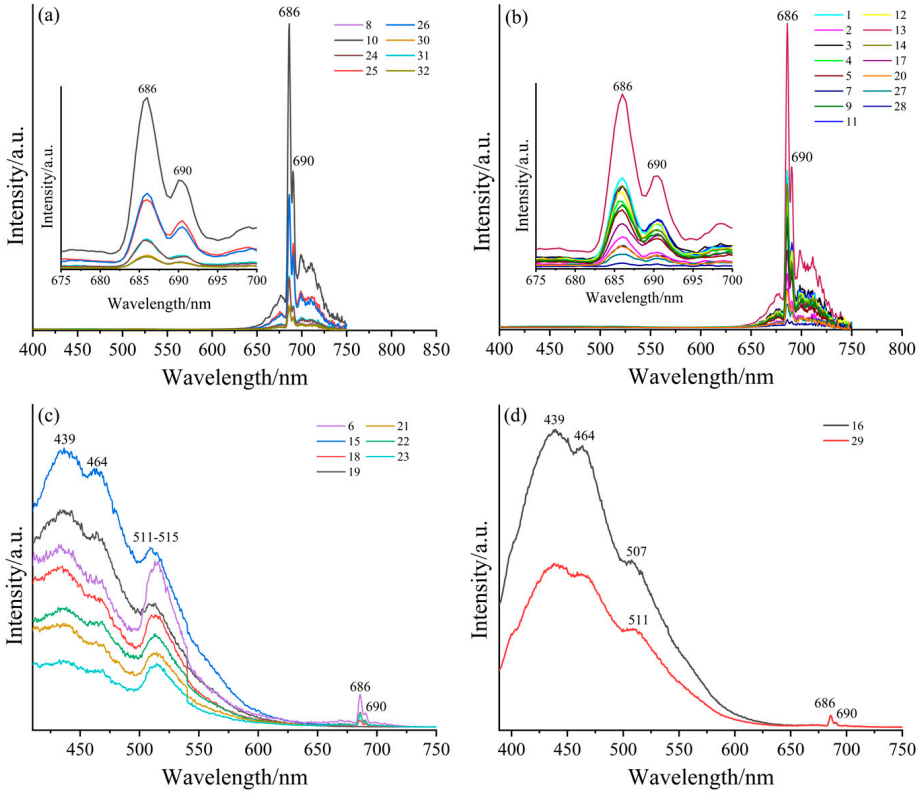


Figure 7. Two-dimensional fluorescence spectra of taaffeites using 369 nm excitation. (**a**) Samples with orange-red fluorescence under LWUV. The red region of fluorescence spectra had been enlarged for better analysis, which placed on the left side. (**b**) Samples with pink fluorescence under LWUV. The red region of fluorescence spectra had been enlarged for better analysis, which placed on the left side. (**c**) Samples with green fluorescence under LWUV. (**d**) Samples with blue-white fluorescence under LWUV.

Table 1. Contents of trace elements in samples with orange-red and pink fluorescence under LWUV (ppmw).

Sample	Cr	V	Ti	Mn	Fe	Color under LWUV
10	32.1	9.83	6.09	27.0	2822	Orange-red
26	109	118	39.9	128	3815	
25	77.2	37.4	13.4	49.5	2826	
31	43.9	29.6	6.59	127	4554	
8	16.8	20.4	3.26	54.0	2405	
24	19	37.4	8.17	142	4766	
30	21.3	24.1	13.0	102	4993	
32	21.1	15.6	15.9	116	5098	
Detection Limits	10.7	0.43	0.79	5.32	91.2	
13	34.3	8.33	5.44	35.9	2399	Pink
3	34.8	11.2	6.94	26.0	2380	
1	33.1	20.5	3.53	67.9	4437	
2	19.6	10.5	7.21	31.8	2624	
11	23.6	29.6	6.31	50.8	3166	
14	45.1	29.9	6.41	131	4777	
12	18.2	7.77	6.51	31.3	2810	
4	30.0	10.6	4.06	27.6	2508	
9	21.8	29.9	4.54	61.0	3320	
5	29.8	30.8	38.8	85.7	4128	
17	19.9	26.7	5.48	54.0	3684	
7	11.4	27.2	5.96	59.1	3569	
27	bdl	11.4	7.43	26.8	1675	
28	bdl	18.3	6.83	45.5	2531	
20	bdl	34.9	11.4	44.3	2658	
Detection Limits	11.2	0.30	1.21	4.29	81.4	

bdl: below detection limit.

Figure 7b shows the two-dimensional fluorescence spectra of the samples with pink fluorescence under LWUV (No. 1, 2, 3, 4, 5, 7, 9, 11, 12, 13, 14, 17, 20, 27, and 28). They also have two prominent peaks (686 nm and 690 nm) in the red region. The peak positions are consistent with the samples with orange-red fluorescence. Compared with the fluorescence intensity and peaks in the two-dimensional fluorescence spectra of the samples with pink fluorescence, there exists a similar relationship with the orange-red fluorescence group. Moreover, Cr^{3+} is the activator of the orange-red fluorescence under LWUV, it is speculated that Cr^{3+} can also cause pink fluorescence in taaffeite under LWUV, and Fe inhibits fluorescence generation.

It should be mentioned that the contents of Cr in samples 20, 27, and 28 are lower than the detection limits, which corresponds with their weak fluorescence (under LWUV). Moreover, since LA-ICP-MS is a destructive testing method and taaffeite is valuable, these samples were only tested at one or two points, which can also affect the results.

3.3.2. Green Fluorescence Group under LWUV

On the right side of Figure 3, the samples presented green fluorescence under LWUV (No. 6, 15, 18, 19, 21, 22, and 23). The fluorescence peaks (Figure 7c) at 439 nm and 464 nm in the blue region are evident in the two-dimensional fluorescence spectra. A peak at 511–515 nm exists in the green region. Additionally, two weak peaks at 686 nm and 690 nm can be observed in the red region.

Table 2 shows the LA-ICP-MS results of the samples with green fluorescence under LWUV. They have similar elemental contents of Mn (91.3–138 ppmw). Mn^{2+} is one of the important causes of mineral fluorescence [20]. It is responsible for the green, yellow, and orange-red luminescence in minerals, and the fluorescence color is related to the position of Mn^{2+} in the crystal structure [19]. For example, the green emission of spinel is connected with Mn^{2+} in the tetrahedral site [23]. Willemite can also emit green fluorescence, which is caused by Mn^{2+} that occupies the tetrahedral site [20,24]. In the structure of taaffeite, Mg^{2+} occupies the tetrahedral position. Due to the same valence and similar ionic radii of Mg^{2+} and Mn^{2+} (0.57 and 0.66 Å, respectively, in 4-coordination) [25], Mn^{2+} is most likely located in the tetrahedral position in taaffeite. Considering the correlation between ionic position and fluorescence color, it can be speculated that a relationship exists between Mn^{2+} and green fluorescence under LWUV. However, the influence of other trace elements cannot be excluded, and it may be caused by a combination of them.

Table 2. Contents of trace elements in samples with green fluorescence under LWUV (ppmw).

Sample	Mn	V	Ti	Cr	Fe
22	114	21.1	11.1	15.2	4019
15	109	17.1	8.58	bdl	4436
19	108	15.1	7.76	bdl	5409
6	138	15.6	9.16	bdl	4137
18	95.0	12.0	11.1	bdl	4197
21	91.3	12.7	13.8	bdl	4271
23	107	16.7	8.23	bdl	4551
Detection Limits	4.29	0.30	1.21	11.2	81.4

bdl: below detection limit.

3.3.3. Blue-white Fluorescence Group under LWUV

Samples 16 and 29 show the blue-white fluorescence under LWUV (Figure 3). In Figure 7d, the two-dimensional fluorescence spectra have prominent peaks at 439 nm and 464 nm in the blue region, a relatively weak peak at 507 nm for sample 16 and 511 nm for sample 29 in the green region, and two very weak peaks at 686 nm and 690 nm in the red region for both samples. By comparison, the sample with relatively intense blue-white fluorescence under LWUV (No. 16) has stronger peaks in the fluorescence spectrum.

As is shown in Table 3, two taaffeite samples with blue-white fluorescence under LWUV show a considerable difference in their Fe contents at 1910 ppmw and 3293 ppmw, respectively. The other trace elements are also similar. Since only two taaffeite samples presented blue-white fluorescence under LWUV, the number of samples was too limited to analyze the correlation between trace element contents, fluorescence color, and fluorescence intensity. Moreover, there is no theoretical support; the reason for the blue-white fluorescence generation is not known, and thus further investigation is needed. However, the comparison still indicates that the presence of Fe inhibits the fluorescence in some way.

Table 3. Contents of trace elements in samples with blue-white fluorescence under LWUV (ppmw).

Sample	Mn	V	Ti	Cr	Fe
16	97.8	24.1	7.64	17.2	1910
29	103	48.7	9.77	bdl	3293
Detection Limits	6.24	0.51	2.24	14.8	94.7

bdl: below detection limit.

4. Conclusions

This work provides information on taaffeites from Mogok, Myanmar, including standard gemological data, images, and Raman spectra of the inclusions, luminescence characteristics, fluorescence spectra features, and trace element data from LA-ICP-MS.

The refractive index of taaffeite samples from Mogok, Myanmar, ranges from 1.713 to 1.729, with the birefringence ranging from 0.001 to 0.006 and the specific gravity ranging from 3.578 to 3.686. These results are consistent with the physical and optical properties of taaffeites from other origins.

The examined taaffeite samples have various internal features, and many of them are distinguished from taaffeites of other origins. The visible inclusions contain irregular inclusions, orange and brown intrusions, black dots and flakes, healed fissures, and tubular and fingerprint inclusions. The mineral inclusions include calcite, forsterite, celestite, dolomite, and graphite. Dolomite is regarded as the characteristic inclusion of taaffeite from Mogok, Myanmar. Large amounts of carbonates indicate that these taaffeites formed in a carbonate metamorphic environment. In addition, CO_2 was also found in these taaffeites.

Taaffeites have specific characteristic fluorescence. The fluorescence colors under LWUV can be divided into four categories: orange-red, pink, green, and blue-white. Using two-dimensional fluorescence spectra, it was found that the samples with orange-red and pink fluorescence had two very strong peaks at 686 nm and 690 nm in the red region. Samples showing green and blue-white fluorescence had strong peaks at 439 nm and 464 nm in the blue region, a relatively weak peak in the green region, and two very weak peaks at 686 nm and 690 nm in the red region. When combined with the chemical composition data from LA-ICP-MS, this suggests that Cr^{3+} is the activator of the orange-red and pink fluorescence, Mn^{2+} is responsible for the green fluorescence, and Fe inhibits the generation of fluorescence.

Author Contributions: Investigation, B.L.; writing—original draft preparation, B.L. and L.Z.; writing—review and editing, Q.Z., B.L., X.L. (Xingtong Li) and X.L. (Xiaojing Lai). All authors have read and agreed to the published version of the manuscript.

Funding: This research was funded by the National Natural Science Foundation of China (NSFC) grant (No. 42002041) and the Fundamental Research Funds for the Central Universities, China University of Geosciences (Wuhan) (No.162301202618) to Xiaojing Lai.

Data Availability Statement: All supporting data and computational details are available on written request. These data are stored by the main author of this article.

Acknowledgments: We would like to thank the mineral collector Xiaokang Xiong for providing us with the taaffeite samples.

Conflicts of Interest: The authors declare no conflict of interest.

References

1. Mills, S.J.; Hatert, F.; Nickel, E.H.; Ferraris, G. The Standardisation of Mineral Group Hierarchies: Application to Recent Nomenclature Proposals. *Eur. J. Mineral.* **2009**, *21*, 1073–1080. [CrossRef]
2. Armbruster, T. Revised Nomenclature of Hogbomite, Nigerite, and Taaffeite Minerals. *Eur. J. Mineral.* **2002**, *14*, 389–395. [CrossRef]
3. Yang, Z.; Ding, K.; De Fourestier, J.; Mao, Q.; Li, H. Ferrotaaffeite-2N'2S, a New Mineral Species, and the Crystal Structure of Fe^{2+}-Rich Magnesiotaaffeite-2N'2S from the Xianghualing Tin-Polymetallic Ore Field, Hunan Province, China. *Can. Mineral.* **2012**, *50*, 21–29. [CrossRef]
4. Chen, J.; Yang, J.; Wang, Q. The Principle of Constructing the Crystal Structures of Nigerite-Taaffeite-Hogbomite and their Related Minerals. *Acta Mineral. Sin.* **2001**, *01*, 19–26. (In Chinese)
5. Gatehouse, B.M.; Grey, I.E. The Crystal Structure of Höegbomite-8H. *Am. Mineral.* **1982**, *67*, 373–380.
6. Malcherek, T.; Schluter, J. Crystal Structure of Cr-bearing $Mg_3BeAl_8O_{16}$, a New Polytype of Magnesiotaaffeite-2N'2S. *Acta Crystallogr. Sect. E Crystallogr. Commun.* **2016**, *72*, 1060–1063. [CrossRef]
7. Leelawatanasuk, T.; Atichat, W.; Thye Sun, T.; Sriprasert, B.; Jakkawanvibul, J. Some Characteristics of Taaffeite from Myanmar. *J. Gemmol.* **2014**, *34*, 144–148. [CrossRef]
8. Schmetzer, K.; Krzemnicki, M.; Hänni, H.A.; Bernhardt, H.-J.; Pettke, T. Gem-quality Taaffeites and Musgravites from Africa. *J. Gemmol.* **2007**, *30*, 367–382. [CrossRef]
9. Schmetzer, K.; Kiefert, L.; Bernhardt, H.-J.; Burford, M.; Gunasekara, D.P. Iron- and Zinc-rich Gem-quality Taaffeites from Sri Lanka. *J. Gemmol.* **2005**, *29*, 290–298. [CrossRef]
10. Schmetzer, K.; Kiefert, L.; Bernhardt, H.-J. Purple to Purplish Red Chromium-bearing Taaffeites. *Gems Gemol.* **2000**, *36*, 50–58. [CrossRef]
11. Peng, Z.; Wang, K. The Crystal Structure of Taaffeite. *Chin. Sci. Bull.* **1963**, *14*, 70–71. (In Chinese)
12. Schmetzer, K.; Kiefert, L.; Bernhardt, H.-J.; Burford, M. Two Remarkable Taaffeite Crystals from Sri Lanka. *J. Gemmol.* **2005**, *29*, 461–466. [CrossRef]
13. Gunawardene, M. Inclusions in Taaffeites from Sri Lanka. *Gems Gemol.* **1984**, *20*, 159–163. [CrossRef]
14. Zaw, K.; Sutherland, L.; Yui, T.-F.; Meffre, S.; Thu, K. Vanadium-rich ruby and sapphire within Mogok Gemfield, Myanmar: Implications for gem color and genesis. *Miner. Depos.* **2014**, *50*, 25–39. [CrossRef]
15. Malíčková, I.; Bačík, P.; Fridrichová, J.; Hanus, R.; Illášová, Ľ.; Štubňa, J.; Furka, D.; Furka, S.; Škoda, R. Optical and Luminescence Spectroscopy of Varicolored Gem Spinel from Mogok, Myanmar and Lục Yên, Vietnam. *Minerals* **2021**, *11*, 169. [CrossRef]
16. Phyo, M.M.; Bieler, E.; Franz, L.; Balmer, W.; Krzemnicki, M.S. Spinel from Mogok, Myanmar—A Detailed Inclusion Study by Raman Microspectroscopy and Scanning Electron Microscopy. *J. Gemmol.* **2019**, *36*, 418–435. [CrossRef]
17. Themelis, T. *Gems & Mines of Mogok: Fascinating Glimpses into the Gemology, Geology and Gem Mining of Mogok, Myanmar (Burma)*; A&T Publishers: Anchorage, AK, USA, 2008.
18. Kiefert, L.; Schmetzer, K. Distinction of Taaffeite and Musgravite. *J. Gemmol.* **1998**, *26*, 165–167. [CrossRef]
19. Gaft, M.; Reisfeld, R.; Panczer, G. *Modern Luminescence Spectroscopy of Minerals and Materials*; Springer: New York, NY, USA, 2015.
20. Marfunin, A.D.S. *Spectroscopy, Luminescence and Radiation Centers in Minerals*; Springer: New York, NY, USA, 1979.
21. Zeug, M.; Nasdala, L.; Chanmuang, N.C.; Hauzenberger, C. Gem Topaz from the Schneckenstein Crag, Saxony, Germany: Mineralogical Characterization and Luminescence. *Gems Gemol.* **2022**, *58*, 2–17. [CrossRef]
22. Wang, C.; Shen, A.H.; Liu, Y. Characterization of Order-Disorder Transition in $MgAl_2O_4$: Cr^{3+} Spinel using Photoluminescence. *J. Lumin.* **2020**, *227*, 117552. [CrossRef]
23. Mohler, R.L.; White, W.B. Influence of Structural Order on the Luminescence of Oxide Spinels: Manganese Activated Spinels. *Mater. Res. Bull.* **1994**, *29*, 1109–1116. [CrossRef]
24. Lojpur, V.; Nikolić, M.G.; Jovanović, D.; Medić, M.; Antić, Ž.; Dramićanin, M.D. Luminescence Thermometry with Zn_2SiO_4: Mn^{2+} powder. *Appl. Phys. Lett.* **2013**, *103*, 141912. [CrossRef]
25. Shannon, R.D. Revised effective ionic radii and systematic studies of interatomic distances in halides and chalcogenides. *Acta Crystallogr. Sect. A* **1976**, *32*, 751–767. [CrossRef]

Disclaimer/Publisher's Note: The statements, opinions and data contained in all publications are solely those of the individual author(s) and contributor(s) and not of MDPI and/or the editor(s). MDPI and/or the editor(s) disclaim responsibility for any injury to people or property resulting from any ideas, methods, instructions or products referred to in the content.